Yuping Wang
Key Laboratory of Power Machinery
and Engineering,
Ministry of Education,
Shanghai Jiao Tong University,
800 Dongchuan Road,
Minhang District,
Shanghai 200240, China
e-mail: linerw@sjtu.edu.cn

Xiaoyi Ding
Key Laboratory of Power Machinery
and Engineering,
Ministry of Education,
Shanghai Jiao Tong University,
800 Dongchuan Road,
Minhang District,
Shanghai 200240, China
e-mail: dingxiaoyi_frank@126.com

Lei Tang
Key Laboratory of Power Machinery
and Engineering,
Ministry of Education,
Shanghai Jiao Tong University,
800 Dongchuan Road,
Minhang District,
Shanghai 200240, China
e-mail: tangleisjtu@163.com

Yiwu Weng[1]
Key Laboratory of Power Machinery
and Engineering,
Ministry of Education,
Shanghai Jiao Tong University,
800 Dongchuan Road,
Minhang District,
Shanghai 200240, China
e-mail: ywweng@sjtu.edu.cn

Effect of Evaporation Temperature on the Performance of Organic Rankine Cycle in Near-Critical Condition

Considering the large variations of working fluid's properties in near-critical region, this paper presents a thermodynamic analysis of the performance of organic Rankine cycle in near-critical condition (NORC) subjected to the influence of evaporation temperature. Three typical organic fluids are selected as working fluids. They are dry R236fa, isentropic R142b, and wet R152a, which are suited for heat source temperature from 395 to 445 K. An iteration calculation method is proposed to calculate the performance parameters of organic Rankine cycle (ORC). The variations of superheat degree, specific absorbed heat, expander inlet pressure, thermal efficiency, and specific net power of these fluids with evaporation temperature are analyzed. It is found that the working fluids in NORC should be superheated because of the large slope variation of the saturated vapor curve in near-critical region. However, the use of dry R236fa or isentropic R142b in NORC can be accepted because of the small superheat degree. The results also indicate that a small variation of evaporation temperature requires a large variation of expander inlet pressure, which may make the system more stable. In addition, due to the large decrease of latent heat in near-critical region, the variation of specific absorbed heat with evaporation temperature is small for NORC. Both specific net power and thermal efficiency for the fluids in NORC increase slightly with the rise of the evaporation temperature, especially for R236fa and R142b. Among the three types of fluids, dry R236fa and isentropic R142b are better suited for NORC. The results are useful for the design and optimization of ORC system in near-critical condition.
[DOI: 10.1115/1.4032238]

Keywords: low-grade heat source, organic Rankine cycle (ORC), near-critical condition, performance, thermodynamics

1 Introduction

Low-grade heat source, such as solar energy, geothermal energy, biomass energy, and waste heat, exists widely in nature and industrial processes. Recently, the power generation from low-grade heat source has been intensively studied. A viable choice for utilizing low-grade heat source is ORC technology [1–3]. The performance of an ORC plant is related to the heat source, working fluid, expander, cycle structure, operation condition, etc. There have been many researches focusing on these influence factors. Concerning the selection of suitable working fluids, Bahaa et al. [4] researched 31 pure working fluids for ORC between 30 °C and 100 °C. Chys et al. [5] studied 11 zeotropic mixtures and calculated the optimal concentrations for heat sources at 150 °C and 200 °C. Bao and Zhao [6] investigated the effect of working fluid on the ORC and carried out a summary of the recommended pure and mixed working fluids for disparate applications. Additionally, Mathias et al. [7] conducted theoretical simulation and practical experiments on a scroll expander. Gu et al. [8] evaluated an ORC plant using a scroll expander and found that

the internal and external entropy generation of evaporator was the main source of the total entropy generation. Zhou et al. [9] performed experiments of an ORC for heat recovery from low-temperature flue gas and investigated the influence of the evaporating pressure, superheat degree, and heat source temperature on the system performance parameters. On the other hand, the optimization of cycle structure was performed, Vetter et al. [10] and Vidhi et al. [11] carried out a detailed investigation on supercritical ORC for instance. Vetter et al. [10] analyzed the cycle characteristics of low-temperature geothermal subcritical and supercritical ORC with different kind of working fluids separately. Vidhi et al. [11] conducted a working fluids selecting process of low-grade geothermal supercritical ORC and suggested that R134a had the best performance. Also, the optimization of operation condition is important. Marion et al. [12] investigated the optimal mass flow rates for different solar radiations. Wang et al. [13] gave special attentions to the optimal operation conditions for different heat source temperatures.

Recently, the optimal evaporation temperature, found by many researchers, is adjacent to the critical temperature of working fluid within the fixed heat source temperature. With the heat source of 90 °C, Pan et al. [14] revealed a better performance for an ORC plant operated nearby critical condition than that of supercritical condition in terms of the amount of power output. Nowak et al. [15] also presented that the ORC of which the evaporation

temperature was near the critical temperature had the highest output power when the heat source temperature was 116 °C. Moreover, Vaja and Gambarotta [16] conducted a specific thermodynamic analysis and found that the optimal evaporating pressure was not far from the critical pressure. Additionally, Trela et al. [17] proposed a method for definition of the near-critical region boundary (NRB) of organic working fluids. They indicated that the determination of NRB was important for the design of heat exchangers in near-critical condition. On the contrary, concerning the large variations of working fluids' properties in near-critical region, some researchers suggested that the evaporation temperature should be limited in the subcritical region [18–20]. The higher pressure limit of ORC set by Drescher and Brüggemann [18] was lower than critical pressure by 0.1 MPa. Delgadeo-Torres and Garcia-Rodriguez [19] proposed that the higher temperature of ORC should be 10–15 °C lower than the critical temperature. The higher temperature limit for R32 was 25 °C lower than its critical temperature in Ref. [20]. However, there was no unique interpretation of these evaporation temperature limits in Refs. [18–20]. By comparatively and systematically studying the relevant papers with respect to this subject, the special phenomena of superheat degree, specific absorbed heat, expander inlet pressure, thermal efficiency, and specific net power of ORC operated nearby critical condition has not been investigated as a whole. Thus, a more comprehensive study should be conducted.

A performance analysis of NORC subjected to the influence of evaporation temperature is conducted in this paper. For this purpose, three typical organic fluids are selected as working fluids. An iteration calculation method is proposed to calculate the performance parameters of these working fluids in ORC. The variations of minimum superheat degree, specific absorbed heat, expander inlet pressure, thermal efficiency, and specific net power of working fluid with evaporation temperature are investigated. These parameters of NORC are compared with those of ORC in subcritical condition (SORC). Furthermore, the relationships between the special variations of these parameters of ORC and the large variation of working fluid's properties in near-critical condition are analyzed.

2 Thermodynamic Analysis Methods

2.1 Description of SORC and NORC. The large variations of physical properties of organic working fluids can be observed in near-critical region. As an example, the variations of density (ρ), specific heat (c_p), dynamic viscosity (μ), and thermal conductivity (λ) of R142b with temperature at pressures of 3.5 MPa and 2.5 MPa are shown in Fig. 1. All properties of R142b are obtained from REFPROP 8.0 [21]. As shown in Fig. 1, the variation of c_p with temperature shows a sharp peak at the saturation temperature
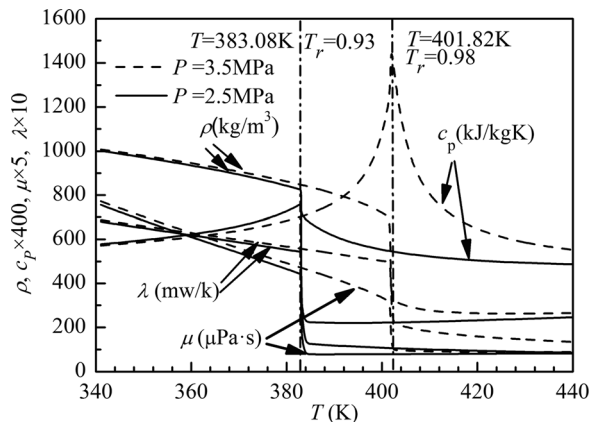
($T = 401.82$ K) which corresponds to $P = 3.5$ MPa and is close to the critical temperature ($T_c = 410.26$ K for R142b), while there is a small peak at the saturation temperature ($T = 383.08$ K) which corresponds to $P = 2.5$ MPa and is far from T_c of R142b. However, other properties including ρ, μ, and λ sharply drop at the saturation temperature. As long as the saturation temperature is close to its critical temperature, the properties concerned show a smaller change. According to the special variations of properties in near-critical region (Fig. 1), the region of working fluid in the temperature–entropy (T–s) diagram below the critical point can be divided into sub- and near-critical region.

In order to analyze the performance of NORC, we compare such performance with that in subcritical condition. The ORC with the evaporation pressure and temperature falling in near-critical region is defined as NORC, while the ORC with the evaporation pressure and temperature falling in subcritical region is defined as SORC. In this paper, the boundary between subcritical region and near-critical region is evaluated with respect to variations of c_p along isobars [17].

2.2 Working Fluids. For heat source temperature from 395 to 445 K, three common working fluids are chosen and they are dry R236fa, isentropic R142b, and wet R152a [6,13]. The critical temperatures of these three fluids are close to each other. Figure 2 shows the T–s diagrams of the fluids. The important properties of the fluids are listed in Table 1. All properties of R236fa, R142b, and R152a are obtained from REFPROP 8.0 [21]. A method proposed by Trela et al. [17] is applied in this paper to calculate the near-critical region boundaries of these fluids. The near-critical region for R236fa is bounded by $0.95 \leq T/T_c \leq 1$ and $0.66 \leq P/P_c \leq 1$. The near-critical region for R142b is bounded by $0.94 \leq T/T_c \leq 1$ and $0.64 \leq P/P_c \leq 1$. The near-critical region for R152a is $0.93 \leq T/T_c \leq 1$ and $0.60 \leq P/P_c \leq 1$. As an example, R142b's near-critical region is shown in Fig. 3.

2.3 Thermodynamic Model. According to the definitions of SORC and NORC, the obvious difference between SORC and NORC is that both the evaporation pressure and temperature of working fluid in NORC are higher than those of SORC. In other words, the extent of the isobaric evaporation process of NORC is smaller than that of SORC. As a matter of fact, this difference does not contribute to the different configurations of NORC and SORC. Both SORC and NORC system have a pump, an evaporator, an expander, and a condenser, as shown in Fig. 4. In general, both SORC and NORC comprise the following four processes: actual compression in a pump, constant pressure heat addition in an evaporator, actual expansion in an expander, and constant pressure heat rejection in a condenser, as shown in Fig. 5. Additionally, the process 3–4 s is the isentropic expansion process. According to the first law of thermodynamic, the mathematical model of each process is given as follows [22–24]:

Fig. 1 Variations of physical properties of R142b in sub- and near-critical region
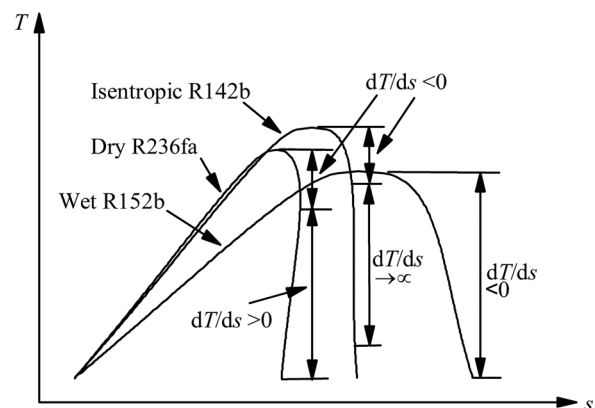
Fig. 2 T–s diagrams of R236fa, R142b, and R152b

Table 1 The physical properties of working fluids

Name	Molecular	Molar mass (g/mol)	T_b (K)	T_c (K)	P_c (MPa)
R236fa	$CF_3CH_2CF_3$	152.04	271.71	398.07	3.20
R142b	CH_3CClF_2	100.49	264.03	410.26	4.12
R152a	CH_3CHF_2	66.05	249.31	386.41	4.52
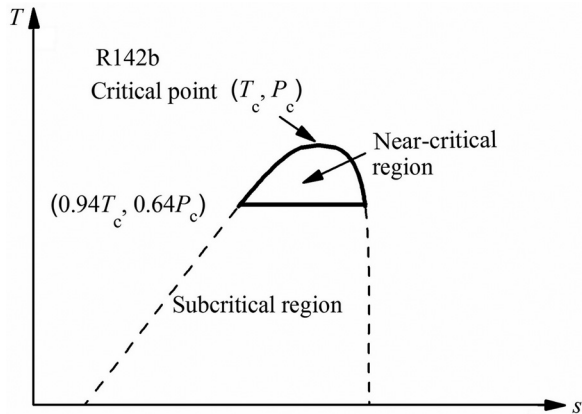
Fig. 3 Schematic diagram of sub- and near-critical region of R142b

Pump (1–2):
The actual power consumption of the pump is

$$W_{\text{pump}} = m_{\text{wf}} v (P_2 - P_1)/\eta_{\text{pump}} \tag{1}$$

Evaporator (2–3):
The working fluid temperature at the evaporator outlet is calculated from

$$T_3 = T_{\text{evp}} + \Delta T_{\text{evp,min}} \tag{2}$$

where $\Delta T_{\text{evp,min}}$ is the minimum superheat degree for working fluid vapor under a given evaporation temperature, which ensures a dry expansion in the expansion process.
The heat absorbed by the working fluid is

$$Q_{\text{evp}} = m_{\text{wf}}(h_3 - h_2) \tag{3}$$
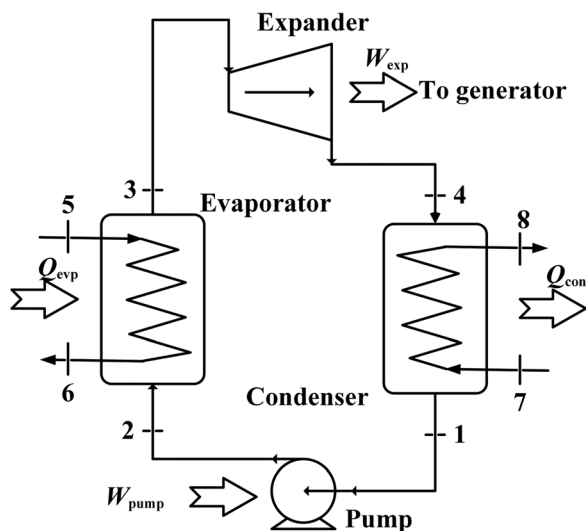
Fig. 4 Schematic diagram of ORC system

Expander (3–4):
The actual power of the expander is

$$W_{\text{exp}} = m_{\text{wf}} \eta_{\text{exp}} (h_3 - h_{4s}) \tag{4}$$

The isentropic efficiency of the expander is expressed as

$$\eta_{\text{exp}} = (h_3 - h_4)/(h_3 - h_{4s}) \tag{5}$$

The specific enthalpy of the working fluid at the expander outlet is calculated as follows:

$$h_4 = h_3 - \eta_{\text{exp}} (h_3 - h_{4s}) \tag{6}$$

In order to check the dryness fraction of working fluid at all points in the expansion process, the actual expansion process is divided into N small expansion segments, as shown in Fig. 6. Each expansion segment has the same pressure drop (ΔP). ΔP is calculated from

$$\Delta P = (P_3 - P_4)/N \tag{7}$$

There are $N+1$ nodes in the whole expansion process. The pressure for each node is calculated through the following equation:

$$p_j = P_3 - (j-1)\Delta P \quad (j = 1, 2, \ldots, N+1) \tag{8}$$

With the assumption of same isentropic efficiency for each expansion segment, the specific enthalpy of the fluid at each expansion segment outlet is calculated as follows:

(a)

(b)
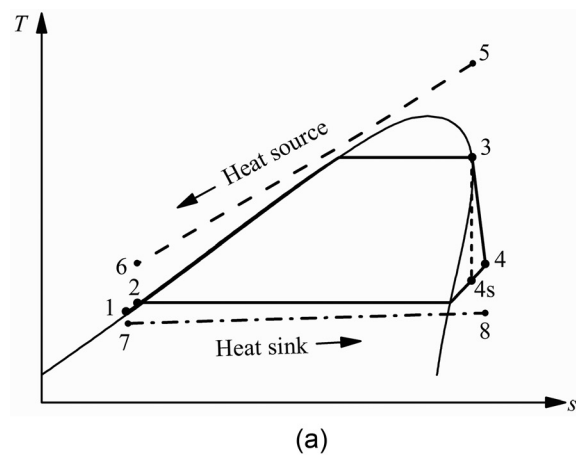
Fig. 5 T–s diagrams of SORC (a) and NORC (b)

$$h_j = h_{j-1} - \eta_{\exp}(h_{j-1} - h_{j,s}) \quad (j = 2, 3, \ldots, N+1) \qquad (9)$$

where $h_{j,s}$ is the specific enthalpy for the isentropic expansion process.

Based on the h_j and p_j, the dryness fraction (x_j) of the fluid at each expansion segment outlet can be obtained from REFPROP 8.0 [21].

Condenser (4–1):

The working fluid temperature at the condenser outlet is calculated from

$$T_1 = T_{\text{con}} - \Delta T_{\text{con}} \qquad (10)$$

The heat released by the working fluid is

$$Q_{\text{con}} = m_{\text{wf}}(h_4 - h_1) \qquad (11)$$

Performance parameters:

The specific absorbed heat of the working fluid in the evaporator is

$$q_{\text{evp}} = Q_{\text{evp}}/m_{\text{wf}} = [m_{\text{wf}}(h_3 - h_2)]/m_{\text{wf}} = (h_3 - h_2) \qquad (12)$$

The specific net power of ORC is calculated through the following equation:

$$w_{\text{net}} = W_{\text{net}}/m_{\text{wf}} = (W_{\text{exp}} - W_{\text{pump}})/m_{\text{wf}} \qquad (13)$$

The thermal efficiency of ORC is calculated as follows:

$$\eta_{\text{th}} = W_{\text{net}}/Q_{\text{evp}} \qquad (14)$$

2.4 Description of Calculation Methods. The minimum superheat degree, specific net power, specific absorbed heat, and thermal efficiency at different evaporation temperatures for these three working fluids are calculated through the iteration calculation method as shown in Fig. 7. In this study, the flow rate of the working fluid in the cycle is set to 1 kg/s. The condensation temperature and subcooling degree of the working fluid in the condenser are 303 K and 5 K, respectively. Additionally, the isentropic efficiencies of the pump and the expander are set to 0.75 and 0.8, respectively. It is noted that the minimum superheat degree of the working fluid for a given evaporation temperature is needed to be iteratively calculated, which can be seen from Fig. 7. The starting value of the superheat degree for the iteration is 0 K. Through the method presented in Sec. 2.3, the dryness fraction of the working fluid vapor at all points in the expansion process can

be checked. If one expansion segment is wet, the iteration program aborts the calculation and starts with a higher superheat degree. The process is repeated until the expansion at each segment has a dry expansion. After obtaining the minimum superheat degree, the performance parameters of working fluids in ORC for a given evaporation temperature can be obtained. The calculations are performed at different evaporation temperatures ranging from 323 K to T_c (where T_c is the critical temperature of each fluid).

3 Results and Discussion

3.1 Minimum Superheat Degree. The superheat degree (ΔT_{evp}) of organic working fluid vapor is important for the performance of ORC. The ΔT_{evp} of working fluid should be the minimum value which just guarantees a dry expansion [6,25]. The minimum superheat degree ($\Delta T_{\text{evp,min}}$) for R236fa, R142b, and R152a at different evaporation temperatures (T_{evp}) ranging from 323 K to T_c (398.07 K for R236fa, 410.26 K for R142b, and 386.41 K for R152a) is given in this study, as shown in Fig. 8.

Figure 8 shows that for dry R236fa in SORC, $\Delta T_{\text{evp,min}}$ is zero. However, for R236fa in NORC, $\Delta T_{\text{evp,min}}$ first remains zero and then increases rapidly when T_{revp} is higher than 0.96. For isentropic R142b in SORC, $\Delta T_{\text{evp,min}}$ first remains zero and then increases when T_{revp} is higher than 0.93. The T_{revp} of 0.93 is close to the near-critical region ($0.94 \leq T_{\text{revp}} \leq 1$). For R142b in NORC, $\Delta T_{\text{evp,min}}$ increases with the increase of evaporation temperature. For R236fa and R142b, the values of $\Delta T_{\text{evp,min}}$ at the critical

Fig. 6 _h–s_ diagram of the expansion process in the expander
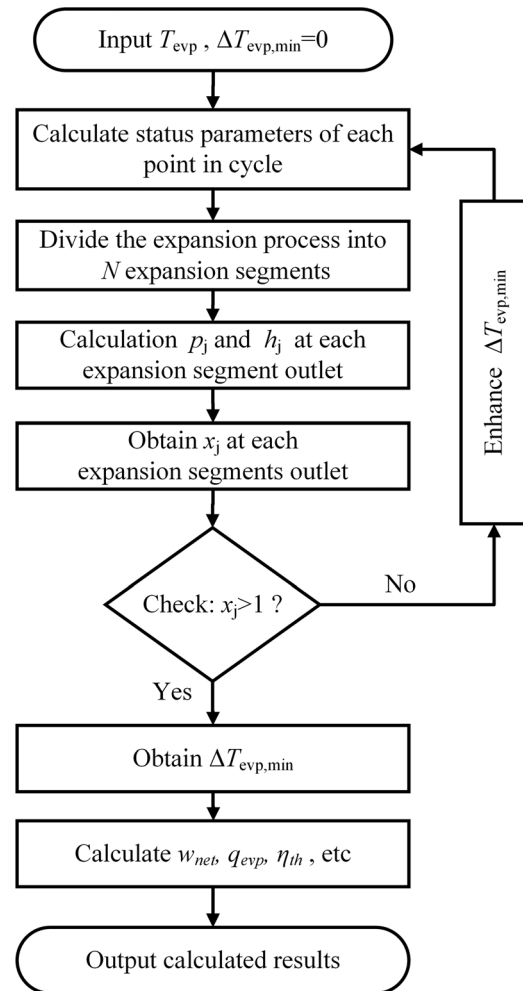
Fig. 7 Calculation of the performance parameters for a given evaporation temperature
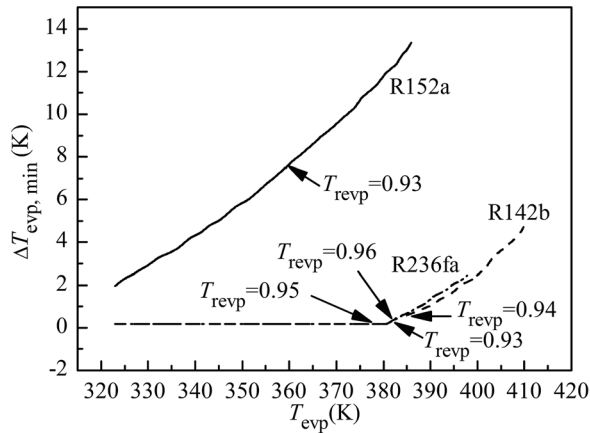
Fig. 8 Variation of minimum superheat degree with evaporation temperature

temperature are about 2.5 and 4.8 K, respectively. The reason for the special variations of the minimum superheat degree for R236fa and R142b in NORC is the large slope variation of the saturated vapor curve in near-critical condition. As shown in Fig. 2, the slopes of the saturated vapor curves for R236fa and R142b in subcritical condition are positive or infinite. R236fa and R142b in saturated vapor can expand and fall in the saturated vapor zone. Therefore, the minimum superheat degree for R236fa and R142b in SORC is mostly zero. However, the slopes of the saturated vapor curve for R236fa and R142b in near-critical condition are negative. R236fa and R142b may cross the two-phase region
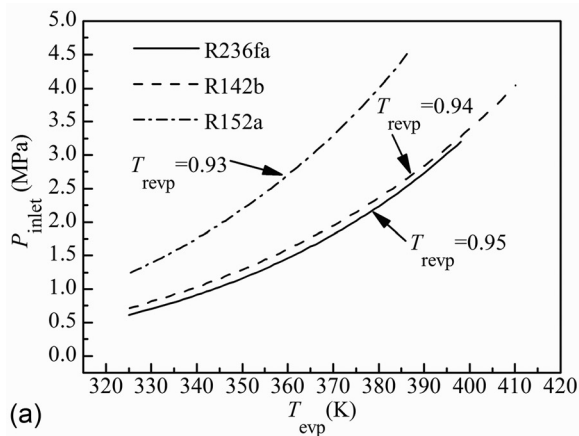
(a)
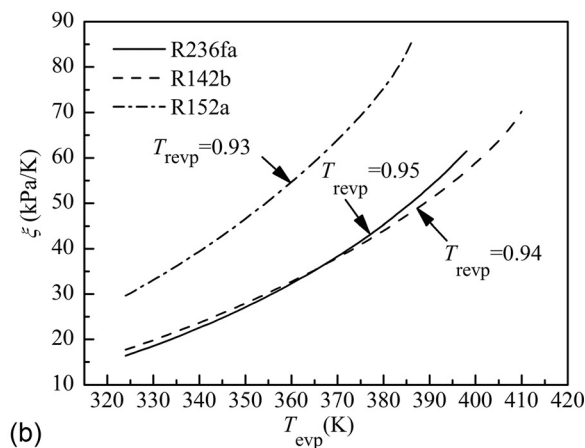
(b)

Fig. 9 Variation of expander inlet pressure (*a*) and its slope (*b*) with evaporation temperature

during the expansion. Therefore, in order to satisfy the dry expansion, R236fa and R142b in NORC should be superheated. In addition, the variation of $\Delta T_{evp,min}$ with evaporation temperature for wet R152a in NORC is similar to that for R152a in SORC. The $\Delta T_{evp,min}$ of R152a increases with an increase in evaporation temperature from 323 K to the critical temperature, because the slope of the saturated vapor curve for R152a remains negative. For R152a, the value of $\Delta T_{evp,min}$ at the critical temperature is about 13.4 K. As previously pointed out, a high value of ΔT_{evp} is not suggested [6,25]. Therefore, the use of dry R236fa or isentropic R142b in NORC can be accepted because of the small superheat degree, while the use of wet R152a in NORC is not recommended because of the high superheat degree.

3.2 Expander Inlet Pressure. Figure 9(*a*) shows the variations of expander inlet pressure (P_{inlet}) for the three working fluids with the evaporation temperature. The expander inlet pressure increases with the increasing evaporation temperature and the maximum value of P_{inlet} is located at the critical temperature of working fluid. It indicates that the expander inlet pressure of NORC is higher than that of SORC. Figure 9(*b*) reports the slopes ($\xi = dP_{inlet}/dT_{evp}$) of the expander inlet pressure curves (Fig. 9(*a*)) under different evaporation temperatures. The slope of the expander inlet pressure curve increases with an increase in evaporation temperature. It demonstrates that the expander inlet pressure of NORC is more sensitive to the evaporation temperature than that of SORC. That is to say, for the working fluid in NORC, a small variation of T_{evp} may bring a large variation of P_{inlet}. Some researchers [6,18–20] thought this special property of working fluid in near-critical condition would make the system unstable. However, this opinion lacks of support on theoretical and experimental results. According to our experimental experiences [8], the evaporation temperature is mostly affected by the expander inlet pressure which depends on the change of working fluid flow rate, expander ratio or load, when the heat source is sufficient. Therefore, it is more reasonable to conclude that a small variation of evaporation temperature for working fluid in NORC requires a large variation of expander inlet pressure. In other words, this special property may make the system more stable. Additionally, among the three working fluids, the P_{inlet} of R152a is the highest at the same T_{evp}, and this is also true for the slope of P_{inlet} curve for R152a. The P_{inlet} of R236fa and R142b are close to each other at the same T_{evp} and so are the slopes of P_{inlet} curves for these two fluids.

3.3 Specific Absorbed Heat. Figure 10 illustrates the variations of the specific absorbed heat (q_{evp}) in the evaporator for these three working fluids with the evaporation temperature. The specific absorbed heat for the fluids in NORC increases more
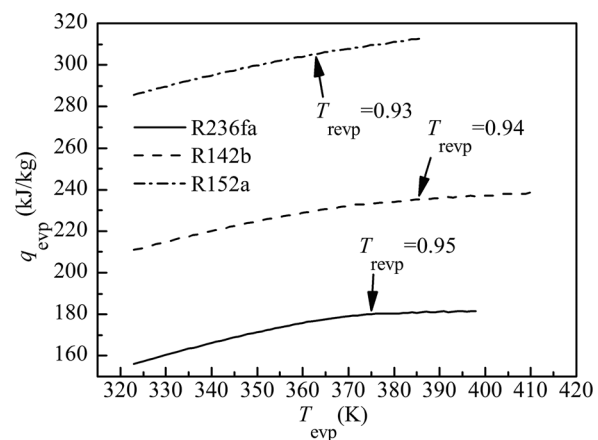
Fig. 10 Variation of specific absorbed heat with evaporation temperature

slightly with the increase of T_{evp} than that in SORC, especially for R236fa and R142b. For R236fa, the average growth rate of q_{evp} in the range of T_{evp} from the lower NRB temperature ($T_{lower,nrb}$ is about 378 K for R236fa) to the critical temperature (T_c is 398.07 K for R236fa) is about 15% of that in the range of T_{evp} from 323 K to $T_{lower,nrb}$. For R142b, the average growth rate of q_{evp} in the range of T_{evp} from $T_{lower,nrb}$ (387 K for R142b) to T_c (410.26 K for R142b) is about 35% of that in the range of T_{evp} from 323 K to $T_{lower,nrb}$. For R152a, the average growth rate of q_{evp} in the range of T_{evp} from $T_{lower,nrb}$ (359 K for R152b) to T_c (386.41 K for R152b) is about 65% of that in the range of T_{evp} from 323 K to $T_{lower,nrb}$. R142b is taken as an example to show the reason for the small variation of specific absorbed heat. The superheat degree of R142b for each evaporation temperature is set to 6 K, which can ensure a dry expansion in the expander for the evaporation temperature from 323 K to the critical temperature. The variation of q_{evp} for R142b with T_{evp} is shown in Fig. 11(a). The variations of q_1, q_2, and q_3 for R142b with T_{evp} are shown in Fig. 11(b). The q_1, q_2, and q_3 are the specific absorbed heat of R142b in the subcooled liquid preheating process, evaporation process, and superheating process, respectively. Figure 11(a) shows that the q_{evp} of R142b first increases and then decreases with the increase of the evaporation temperature. The maximum value is located at $T_{revp} = 0.96$. The reason for this phenomenon is the sharp decrease of q_2 (i.e., latent heat) of the working fluid in near-critical condition. As shown in Fig. 11(b), when T_{revp} is smaller than 0.96, the sum of the ascending rate of q_1 and q_3 is larger than the descending rate of q_2, causing the total absorbed heat to increase continuously. However, when T_{revp} is higher than 0.96, the sum of the ascending rate of $q1$ and $q3$ is smaller than the descending rate of q_2, causing the q_{evp} of R142b to decrease continuously. Therefore, the maximum specific absorbed heat
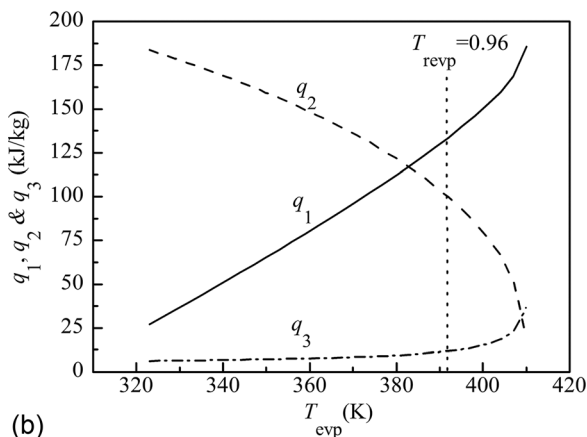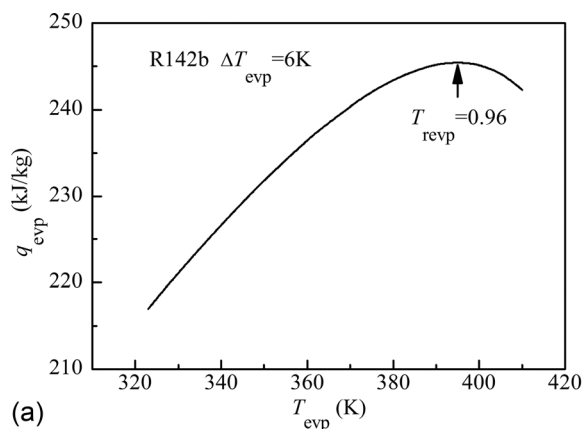
occurs at $T_{revp} = 0.96$. R236fa and R152a are also in the similar trend. Referring to Figs. 3 and 4, it is obvious that the reason for the small variations of q_{evp} for these three working fluids in NORC is the sharp decrease of the working fluids' latent heat in near-critical condition.

The specific absorbed heat in the evaporator decreased slowly with the increasing evaporation temperature [14]. It is contrary to the variations of specific absorbed heat in our study. Pan et al. [14] showed that the evaporator outlet temperature was set to 85 °C and it was avoided that the working fluids expanded into two-phase region. Hence, the superheat degree of the working fluids was the highest at the lowest evaporation temperature and decreased with the increasing evaporation temperature. However, in our study, the superheat degree of the working fluids at different evaporation temperatures is the minimum value which just guarantees a dry expansion. The difference on the superheat degree may cause that the variations of the specific absorbed heat in our study are different from those in Ref. [14].

3.4 Specific Net Power and Thermal Efficiency. Figure 12 shows the variations of specific net power (w_{net}) for R236fa, R142b, and R152a with evaporation temperature. The specific net power of the fluids increases with the rise of evaporation temperature. The specific net power of the fluids in NORC is all higher than that in SORC and all the maximum values of w_{net} are at the critical temperature. However, the average growth rates of w_{net} for the fluids in the range of T_{evp} from $T_{lower,nrb}$ (378 K for R236fa, 387 K for R142b, and 359 K for R152b) to T_c (398.07 K for R236fa, 410.26 K for R142b, and 386.41 K for R152b) are all smaller than those in the range of T_{evp} between 323 K and $T_{lower,nrb}$. It is most obvious for R236fa, as the former is lower than the latter by about 60%. For R142b, the former is smaller than the latter by about 50%. However, this phenomenon is not obvious for R152a, as the former is lower than the latter by about 30%. Since the specific enthalpy of working fluid at the expander inlet mainly depends on the specific absorbed heat in the evaporator when the condensation conditions are fixed, the small variations of the specific net power for the fluids in NORC are mainly a consequence of the small variations of the specific absorbed heat, as shown in Figs. 10 and 12.

Figure 13 reports the variations of thermal efficiency for R236fa, R142b, and R152a with the evaporation temperature. The thermal efficiency of these three fluids increases with the increase of evaporation temperature and has its maximum value at the critical temperature. All the thermal efficiency of the fluids in NORC is higher than that in SORC. Similarly, they vary slightly with the evaporation temperature. For R236fa, R142b, and R152a, the average growth rates of η_{th} in the range of T_{evp} from $T_{lower,nrb}$ to

(a)

(b)

Fig. 11 Variations of q_{evp} (a) and q_1, q_2, and q_3 (b) of R142b with evaporation temperature
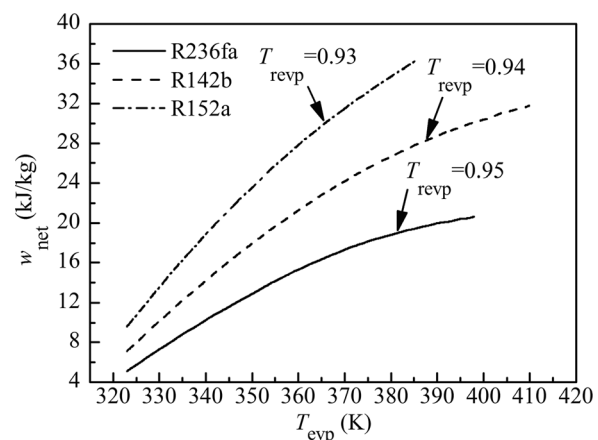
Fig. 12 Variation of specific net power with evaporation temperature
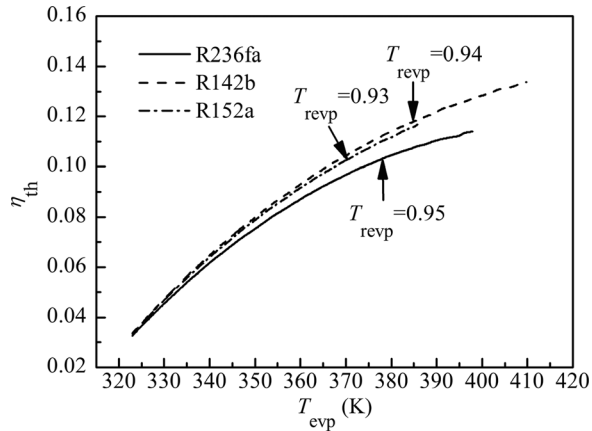
Fig. 13 Variation of thermal efficiency with evaporation temperature

T_c are lower than those in the range of T_{evp} from 323 K to $T_{lower,nrb}$ by about 60%, 55%, and 40%, respectively.

4 Conclusions

The special variations of the performance parameters for dry R236fa, isentropic R142b, and wet R152a in NORC with evaporation temperature have been investigated in this paper. The relations between the special variations of the performance parameters and some working fluid properties are analyzed. The main conclusions are summarized as follows:

(1) Dry R236fa and isentropic R142b in NORC should be superheated. The $\Delta T_{evp,min}$ of R152a increases with an increase in evaporation temperature from 323 K to the critical temperature. The values of $\Delta T_{evp,min}$ at the critical temperature for R236fa, R142b, and R152a are about 2.5, 4.8, and 13.4 K, respectively. Therefore, dry R236fa or isentropic R142b can be adopted in NORC because of the small superheat degree, while wet R152a is not recommended because of the high superheat degree.

(2) The variation of expander inlet pressure of working fluid in NORC with the evaporation temperature is much larger than that in SORC. It indicates that a small variation of evaporation temperature for working fluid in NORC requires a large variation of expander inlet pressure. This special property may make the system performance more stable.

(3) The specific absorbed heat for working fluid in NORC increases more slowly with the rise of the evaporation temperature than that in SORC, especially for R236fa and R142b. For R236fa, the average growth rate of specific absorbed heat with evaporation temperature in near-critical condition is about 15% of that in subcritical condition. For R142b, the former is 35% of the latter. The reason is the sharp decrease of latent heat of the fluid in near-critical condition.

(4) The specific net power of working fluid in NORC is higher than that in SORC. It is true of the thermal efficiency of the fluids in NORC as well. Additionally, both specific net power and thermal efficiency for the fluids in NORC increase slightly with the rise of the evaporation temperature, especially for R236fa and R142b.

It can be concluded that the large variations of working fluid properties have a good effect on the performance of NORC. The specific net power and thermal efficiency vary slowly with the evaporation temperature, which means that the performance of NORC at off-design condition is superior to that of SORC. In addition, among these three working fluids, dry R236fa and isentropic R142b are better suited for NORC.

Nomenclature

c_p = specific heat (kJ/(kg K))
h = enthalpy (J/kg)
m = mass flow rate (kg/s)
N = the number of small expansion segments
p = pressure for each node (Pa)
P = pressure (Pa)
P_c = critical pressure (Pa)
P_{inlet} = expander inlet pressure (Pa)
q = specific absorbed heat (J/kg)
Q = heat (W)
T = temperature (K)
T_b = normal boiling temperature (K)
T_c = critical temperature (K)
T_{evp} = evaporation temperature (K)
$T_{lower,nrb}$ = lower near-critical region boundary temperature (K)
T_r = reduced temperature
$T_r = T/T_c$
T_{revp} = reduced evaporation temperature, $T_{revp} = T_{evp}/T_c$
v = specific volume of working fluid (m^3/kg)
W = power (W)
w_{net} = specific net power (J/kg)
W_{net} = net power (W)
x = dryness fraction of working fluid vapor

Greek Symbols

ΔP = pressure drop in expander (Pa)
ΔT_{con} = degree of subcooling (K)
ΔT_{evp} = superheat degree (K)
$\Delta T_{evp,min}$ = minimum superheat degree (K)
η_{exp} = isentropic efficiency of expander
η_{pump} = isentropic efficiency of pump
η_{th} = thermal efficiency
λ = thermal conductivity (K)
μ = dynamic viscosity (μPa s)
ρ = density (kg/m^3)

Subscripts

c = critical point
con = condenser or condensation
evp = evaporator or evaporation
exp = expander
j = state of working fluid at j node in the expansion process
j,s = state of working fluid for the isentropic expansion process
pump = pump
wf = working fluid
1,2,3,4 = states in system of working fluid
4s = state of isentropic point of working fluid in expander
5, 6 = states in system of heat source
7, 8 = states in system of heat sink

Abbreviations

NORC = ORC in near-critical condition
ORC = organic Rankine cycle
SORC = ORC in subcritical condition

References

[1] Tchanche, B. F., Lambrinos, G., Frangoudakis, A., and Papadakis, G., 2011, "Low-Grade Heat Conversion Into Power Using Organic Rankine Cycles—A Review of Various Applications," Renewable Sustainable Energy Rev., **15**(8), pp. 3963–3979.

[2] Vélez, F., Segovia, J. J., Martín, M. C., Antolín, G., Chejne, F., and Quijano, A., 2012, "A Technical, Economical and Market Review of Organic Rankine Cycles for the Conversion of Low Grade Heat for Power Generation," Renewable Sustainable Energy Rev., **16**(6), pp. 4175–4189.

[3] Walraven, D., Laenen, B., and D'haeseleer, W., 2013, "Comparison of Thermodynamic Cycles for Power Production From Low-Temperature Geothermal Heat Sources," Energy Convers. Manage., **66**, pp. 220–233.

[4] Bahaa, S., Gerald, K., Martin, W., and Johann, F., 2007, "Working Fluids for Low-Temperature Organic Rankine Cycles," Energy, **32**(7), pp. 1210–1221.

[5] Chys, M., Broek, M. V. D., Vanslambrouck, B., and Paepe, M. D., 2012, "Potential of Zeotropic Mixtures as Working Fluids in Organic Rankine Cycles," Energy, **44**(1), pp. 623–632.

[6] Bao, J. J., and Zhao, L., 2013, "A Review of Working Fluid and Expander Selections for Organic Rankine Cycle," Renewable Sustainable Energy Rev., **24**, pp. 325–342.

[7] Mathias, J. A., Johnston, J. R., Cao, J., Priedeman, D. K., and Christensen, R. N., 2009, "Experimental Testing of Gerotor and Scroll Expanders Used in, and Energetic and Exergetic Modeling of, an Organic Rankine Cycle," ASME J. Energy Resour. Technol., **131**(1), p. 012201.

[8] Gu, W., Weng, Y. W., Wang, Y., and Zheng, B., 2009, "Theoretical and Experimental Investigation of an Organic Rankine Cycle for a Waste Heat Recovery System," Inst. Mech. Eng. A-J, **223**(5), pp. 523–533.

[9] Zhou, N. J., Wang, X. Y., Chen, Z., and Wang, Z. Q., 2013, "Experimental Study on Organic Rankine Cycle for Waste Heat Recovery From Low-Temperature Flue Gas," Energy, **55**(15), pp. 216–225.

[10] Vetter, C., Wiemer, H. J., and Kuhn, D., 2013, "Comparison of Sub- and Supercritical Organic Rankine Cycles for Power Generation From Low-Temperature/Low-Enthalpy Geothermal Wells, Considering Specific Net Power Output and Efficiency," Appl. Therm. Eng., **51**(1–2), pp. 871–879.

[11] Vidhi, R., Kuravi, S., Goswami, D. Y., Stefanakos, E., and Sabau, A. S., 2013, "Organic Fluids in a Supercritical Rankine Cycle for Low Temperature Power Generation," J. Energy Resour., **135**(4), pp. 1–9.

[12] Marion, M., Voicu, I., and Tiffonnet, A. L., 2012, "Study and Optimization of a Solar Subcritical Organic Rankine Cycle," Renewable Energy, **48**, pp. 100–109.

[13] Wang, D. X., Ling, X., Peng, H., Liu, L., and Tao, L. L., 2013, "Efficiency and Optimal Performance Evaluation of Organic Rankine Cycle for Low Grade Waste Heat Power Generation," Energy, **50**(1), pp. 343–352.

[14] Pan, L. H., Wang, H. X., and Shi, W. X., 2012, "Performance Analysis in Near-Critical Conditions of Organic Rankine Cycle," Energy, **37**(1), pp. 281–286.

[15] Nowak, W., Borsukiewicz-Gozdur, A., and Wisniewsk, S., 2012, "Influence of Working Fluid Evaporation Temperature in the Near-Critical Point Region on the Effectiveness of ORC Power Plant Operation," Arch. Thermodyn., **33**(3), pp. 73–83.

[16] Vaja, I., and Gambarotta, A., 2010, "Internal Combustion Engine (ICE) Bottoming With Organic Rankine Cycles (ORCs)," Energy, **35**(2), pp. 1084–1093.

[17] Trela, M., Kwidzinski, K., and Butrymowicz, D., 2011, "A Definition of Near-Critical Region Based on Heat Capacity Variation in Transcritical Heat Exchangers," Arch. Thermodyn., **32**(2), pp. 55–68.

[18] Drescher, U., and Brüggemann, D., 2007, "Fluid Selection for the Organic Rankine Cycle (ORC) in Biomass Power and Heat plants," Appl. Therm. Eng., **27**(1), pp. 223–228.

[19] Delgadeo-Torres, A. M., and Garcia-Rodriguez, L., 2007, "Preliminary Assessment of Solar Organic Rankine Cycles for Driving a Desalination System," Desalination, **216**(1–3), pp. 252–75.

[20] Rayegan, R., and Tao, Y. X., 2011, "A Procedure to Select Working Fluids for Solar Organic Rankine Cycles (ORCs)," Renewable Energy, **36**(2), pp. 659–670.

[21] NIST, 2010, *NIST Standard Reference Database 23: Reference Fluid Thermodynamic and Transport Properties-REFPROP*, National Institute of Standards and Technology, Gaithersburg, CO.

[22] Yunus, A. C., and Michael, A. B., 2006, *Thermodynamics: An Engineering Approach*, 5th ed., McGraw-Hill College, Boston, MA.

[23] Li, M. Q., Wang, J. F., He, W. F., Wang, B., Ma, S. L., and Dai, Y. P., 2013, "Experimental Evaluation of the Regenerative and Basic Organic Rankine Cycle for Low-Grade Heat Source Utilization," J. Energy Eng., **139**(3), pp. 190–197.

[24] Li, Y. R., Wang, J. N., and Du, M. T., 2012, "Influence of Coupled Pinch Point Temperature Difference and Evaporation Temperature on Performance of Organic Rankine Cycle," Energy, **42**(1), pp. 503–509.

[25] Mago, P. J., Chamra, L. M., Srinivasan, K., and Somayaji, C., 2008, "An Examination of Regenerative Organic Rankine Cycles Using Dry Fluids," Appl. Therm. Eng., **28**(8–9), pp. 998–1007.